# CHAPTER 3

# METHODOLOGY

## 3.1 Introduction

In this chapter the over excitation current and magnetizing inrush current is studied. Then to make the restraint current, general algorithm and block diagram; benefits of each one (restraining or blocking) is investigated. Meanwhile in the case of over excitation or magnetizing inrush current, how to avoid of mal-operation and make of restraint current for protection relay operation is studied.

Finally, a discussion about restricted earth fault algorithms, advantages and disadvantages of each one is presented.

## 3.2 Magnetizing inrush current

Magnetizing inrush current is a phenomenon that can cause mal operation in protection relays. If the primary of a transformer is connected to the source and the secondary of winding is connected to loads, magnetizing inrush current flows from the supply to the primary winding while there is no current or much smaller load current flowing out of transformer secondary winding (IEEE, 2008a). In fact, magnetizing inrush current occurs when the polarity and magnitude of residual flux opposites of the polarity and magnitude of the ideal instantaneous value of steady state flux (Guzman, et al., 2004; IEEE, 2008a). Figure 3.1 shows the wave form of instantaneous voltage and inrush current according to the time. In this figure, it can be seen that inrush current usually is positive wave.

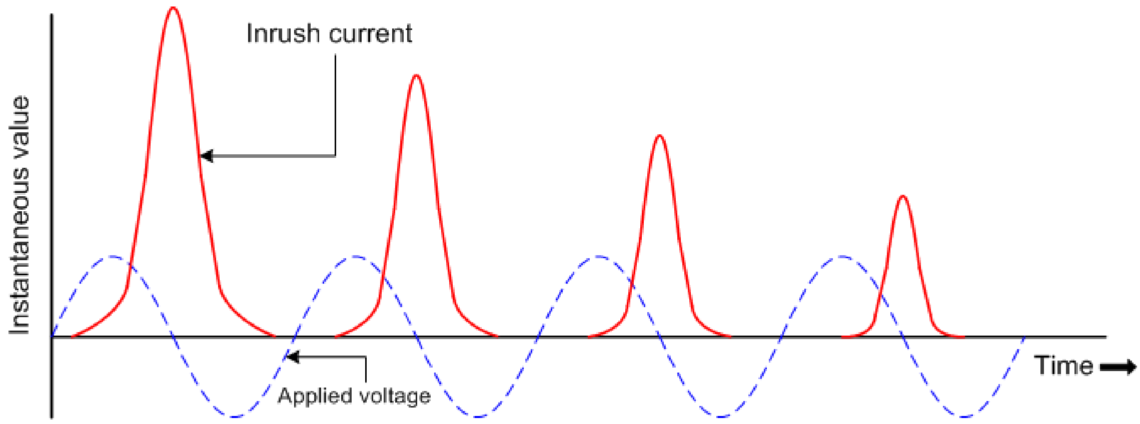


Figure 3.1: Typical magnetizing inrush current wave form (IEEE, 2008a).

The causes of magnetizing inrush current are (Guzman, et al., 2004; IEEE, 2008a; Kasztenny & Kulidjian, 2000):

1. Energizing transformer
2. Occurrence of an external fault
3. Voltage recovery after clearing a fault
4. Fault changing (for example single line to ground fault changes to double line to ground fault)
5. Energizing a transformer in parallel with an in-service transformer
6. Out of phase synchronizing.

And the main characteristics of inrush current are:

1. It generally contains DC offset, odd and even harmonics
2. Typically composed of unipolar or bipolar pulses, separated by very low current values
3. Magnitude of peak value of unipolar inrush current decreases very slowly. This time constant is much greater than the dc offset of fault decays time.
4. Second harmonic constant starts at low values and increases as the inrush current decreases

5. If the relay CTs are connect as a delta connection, then the current is subtracted and (Guzman, J.Alture, & Benmonyal, 2004):
    - DC component is subtracted
    - Fundamental component is added at 60°
    - Second harmonic is added at 120°
    - 3rd harmonic is added at 180°which means it is canceled.

## 3.3 Reason of inrush current

The winding of transformer is linked magnetically by the flux in the transformer core. Supplying the voltage to the transformer drives the flux in the transformer core. By increasing in the exciting voltage, the flux increases in the core. To maintain this additional flux, which it may be passed the knee point of flux curve of transformer, the transformer draws more current that can be more than full load current of transformer windings. This additional current is the inrush current which supplies the magnetizing branch of the transformer (Hunt, Schaefer, & Bentert, 2007).

To show magnetizing inrush current, the single phase equivalent transformer circuit is shown. Assume that the transformer ratio is 1:1. The $I_1$ and $I_2$ are equal except $I_1$ contains small magnetizing current. When the supply voltage increases, the core flux increases hence the magnetizing branch current increases thus $I_1 >> I_2$ (Hunt, et al., 2007; Sen, 2007).

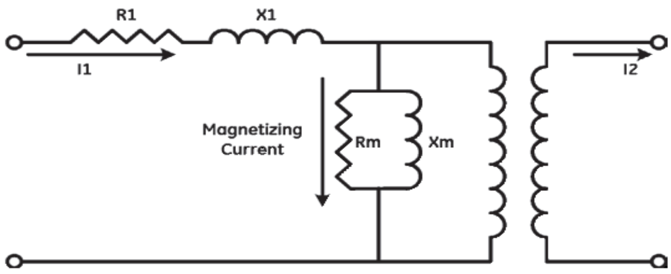


Figure 3.2: Transformer single phase equivalent circuit (Hunt, Schaefer, 2007).

A review of ac excitation of magnetic field and characteristics helps to understand the reasons of inrush current. If the excitation voltage is sinusoidal then the core flux is:

$$\phi(t) = \phi_{max} \sin \omega t \tag{3.1}$$

where:

$\phi_{max}$ is the magnitude of flux

$\omega$ is angular frequency

From Faraday's law, the induced voltage is

$$e(t) = N\frac{d\Phi}{\mathrm{dt}} = N\Phi_{\max}\omega\cos\omega \mathrm{t} = \mathrm{E}_{\max}\cos\omega t \tag{3.2}$$

The root means square of induced voltage is

$$E_{RMS} = \frac{E_{\max}}{\sqrt{2}} = \frac{N\omega\Phi_{\max}}{\sqrt{2}} = 4.44Nf\Phi_{\max} \tag{3.3}$$

Where

f is supply frequency

N is the number of winding turns

If the residual flux exists and it produces the hysteresis loop, the relation between the exciting voltage e, the flux of core $\phi$, and the exciting current $i_\phi$ is shown at figure 3.3. figure 3.3 shows the relation between excited current and magnetic hysteresis loop.

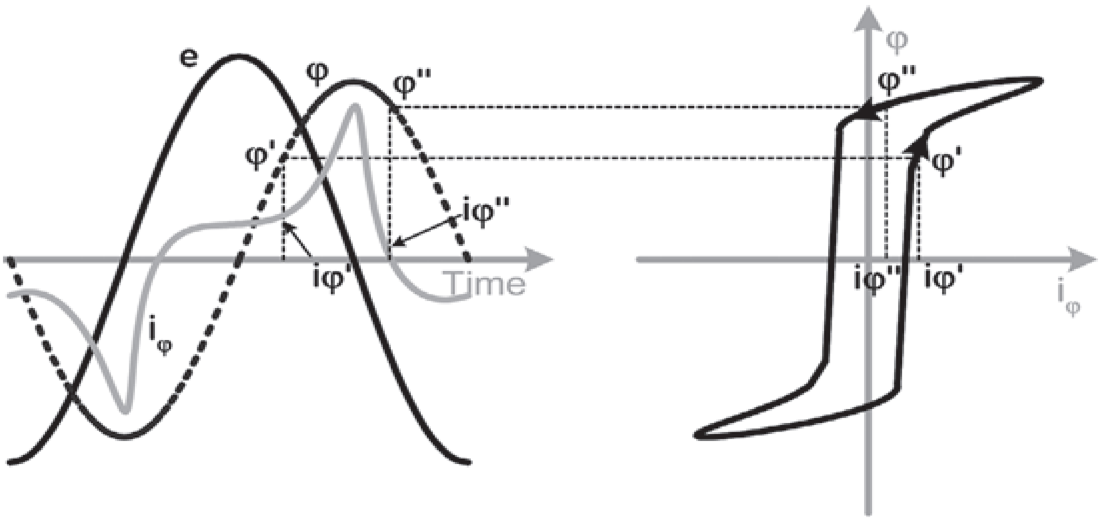


Figure 3.3: Core excitation of transformer (Hunt, Schaefer, & Bentert, 2007).

Figure 3.3 shows that though the voltage e(t) is sinusoidal, the $I_\phi$ is not sinusoidal. A reviewing on hysteresis loop identifies the relation between magnetic flux density B and magnetic flux intensity H. Assume a core does not contain flux. Magnetic flux intensity slowly increases when current increase. When the current decreases magnetic flux intensity also decreases, some flux remain in the transformer core that called residual flux density (Hunt, et al., 2007; Sen, 2007).

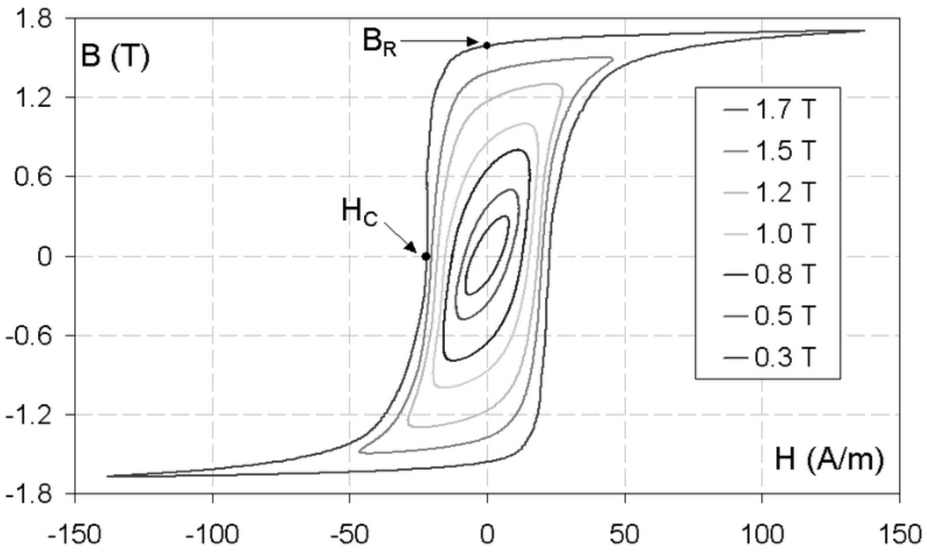


Figure 3.4: Hysteresis loop (Hunt, Schaefer, & Bentert, 2007).

The formulas show the relation between I and H, B and H are

$$\oint H.dl = i \tag{3.4}$$

$$B = \mu_r \mu_0 H \text{ (weber/m}^2\text{) or (tesla)} \tag{3.5}$$

Where

$\mu_r$ is relative permability

$\mu_0$ is free space permability

At this moment, the transformer core has residual flux. These formulas are used at the coming sections for defining of magnetic reasons of inrush current. The factors that influence the magnitude and duration of the inrush current are (Kasztenny & Kulidjian, 2000):

a. *Size of the transformer*; the time constant for decaying of inrush current is in the region of 0.1 second for small transformer (below 100KVA) and in the range of 1 second for larger transformer. The magnitude of peak current of inrush current in small transformer is higher than the large transformer however the duration of inrush current in large transformer is longer.
b. *Impedance of the system from side of transformer is energized;* the total impedance which is seemed from supply till magnetizing impedance helps to dampen of the inrush current. This is why transformers which are located near the generator experience much larger inrush currents than transformers are away from generator.
c. *Core material;* the magnetizing inrush current is larger while the saturation point of core is lower. Figure 3.5 illustrates the relation of inrush current by core magnetic curve.

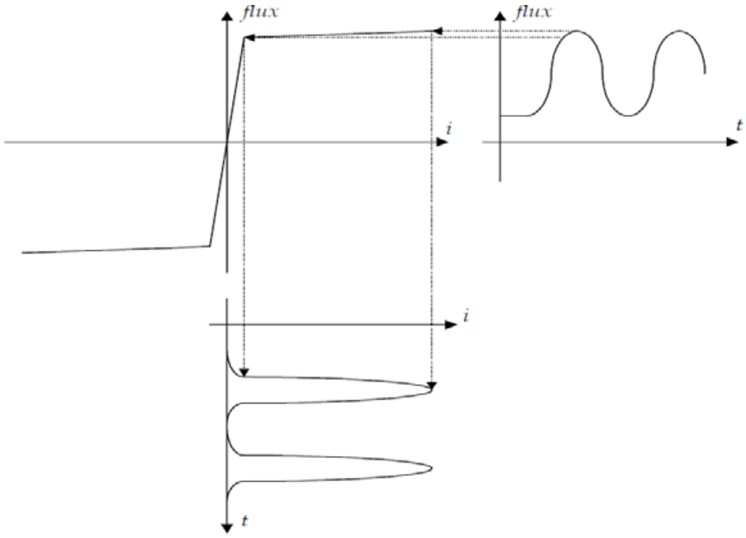


Figure 3.5: Relation of the magnetizing inrush current and core material (Kasztenny & Kulidjian, 2000).

d. *Remanence flux in the core;* from the equations 3.4 and 3.5, whatever residual flux is gone increasing thus the inrush current increases.

e. *The way that transformer is switched in;* the magnitude of inrush current is influenced by the area between core and windings. The inrush current is higher when the inner winding is energized first. Approximately, transformer with conventional steel core may reach inrush current of 5 to 10 times rated value of the outer windings current when it is energized first, instead of 10 to 20 times of rated current when the inner winding is energized. Due to installation coordination, the lower voltage windings are installed near to core and high voltage windings are installed outer, thus energizing from lower voltage reaches to the high inrush current.

f. *Point of wave;* the position of voltage wave form and time of switch in of the transformer is a factor which defines the magnitude of inrush current.

For the switching supply voltage angle, suppose that the voltage is

$$v(t) = V_M \sin(\omega t+\Theta) \tag{3.6}$$

Assume supply voltage is switched in at 90°, thus

$v(t) = V_M \sin(\omega t+90) = V_M \cos \omega t$

From equations 3.2 and v(t) at 90°, therefore

$$\phi_{max} = \frac{V_{max}}{\omega N}$$

Thus the flux is equal to steady state. But if the supply voltage is applied at zero degree

$v(t) = V_M \sin \omega t$

For the first half cycle is given as below

$$\phi(t) = \frac{1}{N}\int_0^{\pi/\omega} V_M \sin \omega t dt = -\frac{V_M}{\omega N}\cos \omega t_0^{\pi/\omega} = -\frac{V_M}{\omega N}[(-1)-(1)]$$

$$\phi_{max} = \frac{2V_{max}}{\omega N}$$

It illustrates that when supply voltage is applied at zero degree, the maximum flux is equal two times of steady state flux and it can produce large amount of current [35].

Also another phase displacement which is important is the phase displacement between voltage and flux. According to the equation 3.2, it is assumed that the phase shifting between voltage and flux $\Theta$ is given

$$e(t) = E_{max} \cos(\omega t-\Theta) \quad (3.7)$$

$$\phi(t) = \phi_{max} \sin(\omega t-\Theta)+\phi_{max} \sin(\Theta) \quad (3.8)$$

If the core contains residual flux, it is added to equation 3.8, thus

$$\phi(t) = \phi_{max} \sin(\omega t-\Theta)+\phi_{max} \sin(\Theta)+ \phi_{residual} \quad (3.9)$$

Figure 3.6 shows the phase displacement between voltage wave form and flux wave

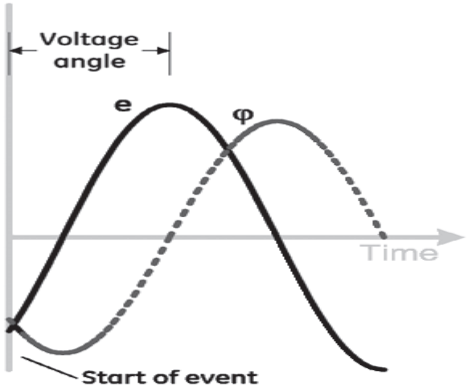


Figure 3.6: Voltage angle during magnetizing (Hunt, Schaefer, & Bentert, 2007).

When the phase displacement between voltage and flux is zero, according to the equation 3.8 there is no flux offset and the fully offset happens when the Ɵ equals to 90°. Maximum saturation of transformer core occurs when the Ɵ equals to 90° or flux is fully offset. Figure 3.7 shows the flux and voltage wave forms when the flux is fully offset or Ɵ=90°.

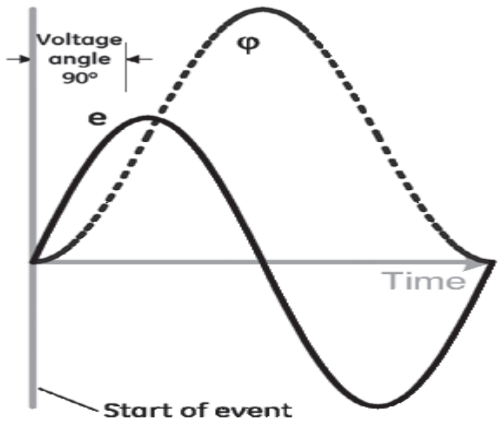


Figure 3.7: Phase displacement 90° between voltage and flux (Hunt, Schaefer, & Bentert, 2007).

According to the sign of remanent flux, the flux can be more or less than value and it can change core condition to the saturation area. Figure 3.8 shows the difference between the positive and negative remanent flux at phase displacement of 90°.

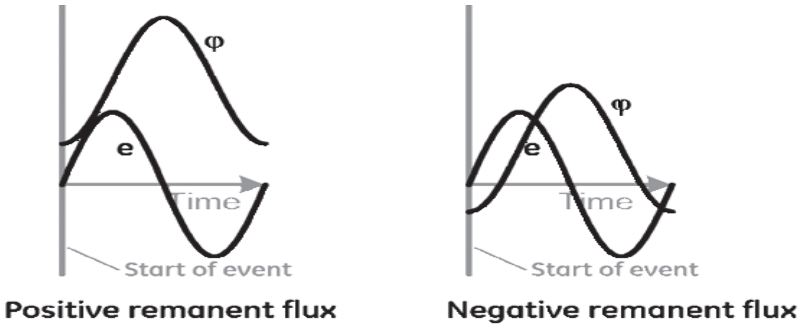


Figure 3.8: Positive and negative remanent flux at 90° angle (Hunt, Schaefer, & Bentert, 2007).

According to (Ling & Basak, 1989), numerical method is used to identify how 2$^{nd}$ harmonic magnitude at different switching time varies. The numerical method to identify the maximum magnitude of 2$^{nd}$ harmonic at different time switching is based on partial change of flux density ($dB_c(t)$), at various time intervals (dt) (Ling & Basak, 1989).

$$dB_c(dt) = \frac{1}{K}[(V_m \sin(\omega t + \theta)dt) - (RI(t)dt) - (L_s dI)] \quad (3.10)$$

$$K = \frac{N[A_c + A_a l_i]}{U_r(t) l_w} \quad (3.11)$$

$$B_c(t + dt) = B_c(dt) + dB_c(dt) \quad (3.12)$$

($B_c$=$B_r$ at t=0)

Where

$B_c$ is transformer core flux density (Tesla)

$B_r$ is residual flux density (Tesla)

$V_m$ is peak source voltage (volt)

N is the winding turns

ϴ is the angle of switching (radian)

R is the total circuit resistance

$L_s$ is the source inductance (henry)

$A_a$ is the air cross section area ($m^2$)

$A_c$ is the core cross section area ($m^2$)

$l_i$ is the core mean path length (m)

$l_w$ is the energizing winding length (m)

$U_r$ is the permeability

I is the magnetizing current (amp.)

$U_r$(t) and I(t) are defined according to the B/H curve. If the small part of B/H curve has chosen, each section can be replaced approximately by a straight line. Then H(t) can be obtained

$$H(t) = \frac{[(B(t) - B_{(n-1)}][H_{(n)} - H_{(n-1)}]}{[B_{(n)} - B_{(n-1)}]} + H_{(n-1)} \qquad (3.13)$$

According to the equations 3.11, 3.12 and 3.13 the B/H curve sample from (Ling & Basak, 1989) is shown in figure 3.9 illustrates the relation between B and H and how it can be approximately changed to a straight line from a curve. Figure 3.10 shows the magnitude of $2^{nd}$ harmonic which is the largest harmonic at inrush current. According to the part 3.3-f this figure proves mathematically that the worth condition occurs during switching at zero degree. While the transformer switching at 90 degree voltage wave form, maximum flux is like flux of the steady state condition.

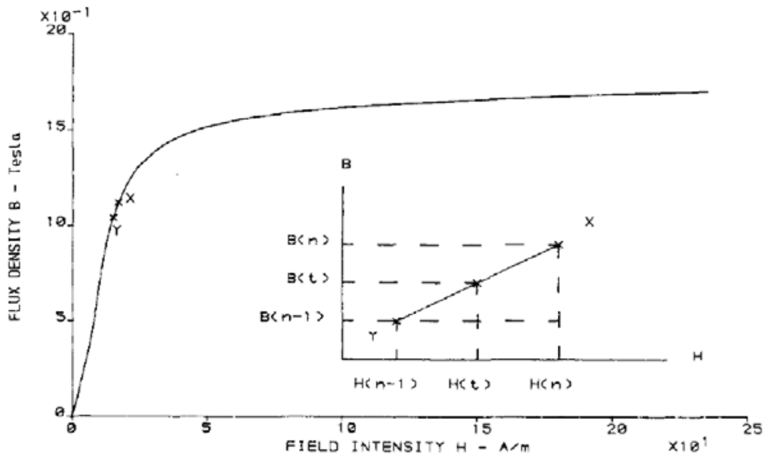


Figure 3.9: B/H curve (Ling & Basak, 1989).

Figure 3.10 shows the magnitude of $2^{nd}$ harmonic according to the time and switching angle.

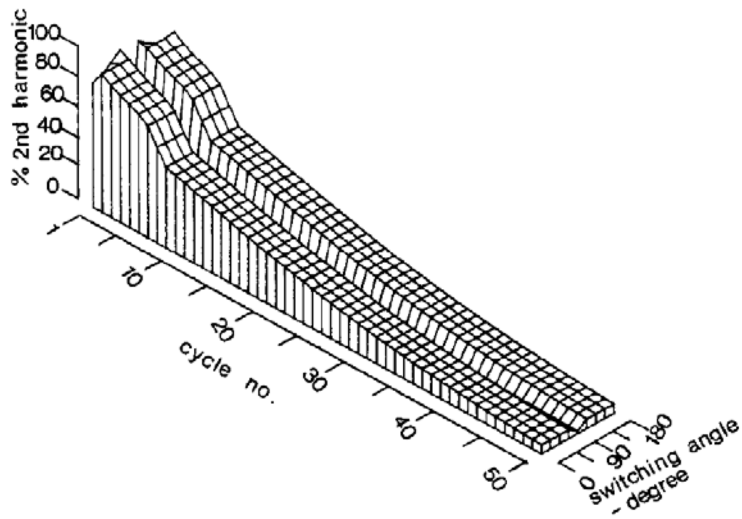


Figure 3.10: Effect of switching angles in the percentage of second harmonic (Ling & Basak, 1989).

The important point in figure 3.10 is that the largest magnitude of $2^{nd}$ harmonic percentage is not at the first cycle. $2^{nd}$ harmonic at the first 10 cycles has the largest magnitude and it is important at REF relay restraining during inrush current.

For applied sinusoidal voltage, the flux density is sinusoidal, thus (Kulkarni & Khaparde, 2004):

$$V_P \sin(\omega t + \theta) = i_o R_1 + N_1 \frac{d\phi_m}{dt} \tag{3.14}$$

Where

$V_p$ is peak value of the supply voltage

$\Theta$ is the angle of voltage that transformer switch on

$i_o$ is the instantaneous of the magnetizing current

$\phi_m$ is the instantaneous flux at time t

$R_1$ is the primary winding resistance

$N_1$ is the primary winding turns

By assuming the leaner magnetic characteristics and initial condition of t=0 and $\phi_m = \pm\phi_r$ (residual flux), thus

$$\phi_m = (\phi_{mp} \cos\theta \pm \phi_r) e^{\frac{-R_1 t}{L_1}} - \phi_{mp} \cos(\omega t + \theta) \tag{3.15}$$

Where, $\phi_{mp}$ is the maximum flux value. Figure 3.11 shows the energized transformer flux wave form. It illustrate that is has a dc component decaying that represents time constant $R_1/L_1$ part and a steady state AC component which is represented at $-\phi_{mp} \cos(\omega t + \theta)$

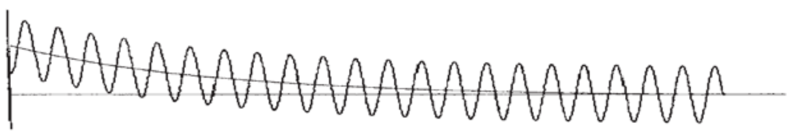

Figure 3.11: Flux wave.

Solving equation 3.14 and 3.15 and using Fourier transform illustrates that the current of inrush has all even harmonics that the 2nd harmonic has largest magnitude because of large DC component.

According to the equation 3.15, the general inrush current is (Ramsis girgis, 2001)

$$\frac{\sqrt{2}U}{Z_t}[\sin(\omega t-\theta)-e^{\frac{-(t-t_0)}{\tau}}\sin\alpha]K_W.K_S \tag{3.16}$$

Where

U is applied voltage

$Z_t$ is total impedance

ϕ is energizing angle

$t_o$ is time of core saturates (function of $B_R$, $B_S$, $B_N$, ϕ)

$B_R$ is residual flux density

$B_S$ is saturation flux density

$B_N$ is normal flux density

t is time constant of transformer

α function of $t_0$

$K_W$ account of the three winding connection

$K_S$ account for short circuit power of network

And the peak value of inrush current is (RS Girgis, et al., 2007; Mekic, et al., 2006)

$$I_{pk}=\frac{\sqrt{2}U}{\sqrt{(\omega.L)^2+R^2}}[\frac{2B_N+B_R-B_S}{B_N}] \tag{3.17}$$

## 3.4 Discrimination between fault current and inrush current

There are different methods to distinguish between fault current and magnetizing inrush current. These methods are incorporated the protection devices to prevent mal-operation. The conventional way to distinguish between fault current and inrush current is the principle of second harmonic and dead angle which are influenced many factors like CT saturation (Jiandong, Chang, & Jianming, 2009).

### 3.4.1 Improved Fourier series (half cycle Fourier series)

One way of distinguish between the fault current and inrush current is using half cycle Fourier series (Jiandong, Chang, & Jianming, 2009). The most important part in the half cycle Fourier transform is the derivation of fundamental current component instead of full wave Fourier transform analysis reflects the synthesis of wave form in one cycle (Jiandong, Chang, & Jianming, 2009). According to the Mann-Morrison half cycle Fourier transform, imaginary part of fundamental current is

$$I_{\mathrm{Im}}(k) = \frac{I_{\mathrm{Re}}(k+1) - I_{\mathrm{Re}}(k-1)}{2\sin(\Delta\theta)} \tag{3.18}$$

Where

$I_{Re}(k)$ is the real part of fundamental current

k is the sampling point

$\Delta\Theta$ is the sampling interval

The peak value of fundamental current is

$$I_1(k) = \sqrt{I_{\mathrm{Re}}^2(k) + I_{\mathrm{Im}}^2(k)} \tag{3.19}$$

$$I'_k = \frac{I_k}{\bar{I}} \qquad (k = 1,2,3,..,N) \tag{3.20}$$

Where $\bar{I}$ is the mean value of $I_1, I_2, \ldots, I_N$, then the parameter D is defined as:

$$D = \frac{1}{N}[(I'_1 - 1)^2 + (I'_2 - 1)^2 + \ldots + (I'_N - 1)^2] \tag{3.21}$$

Parameter D shows the variance of fundamental current's peak value. According to the D, inrush current is defined (Jiandong, Chang, & Jianming, 2009):

- If $D > \varepsilon$, differential current is inrush current
- If $D < \varepsilon$, differential current should be fault current

  $\varepsilon$ is a small value about 0.05.

### 3.4.2 Using wavelet transform

Another way of distinguish between fault current and inrush current is using the wavelet transform. "a wavelet transform (WT) expands a signal not in terms of a trigonometric polynomial but by wavelet, generated using the translation(shift in time)and dilation(compression in time) of a fixed wavelet function called mother wavelet" (Youssef, 2002).

Reference (Mao & Aggarwal, 2000) suggests an algorithm for discrimination between internal fault and inrush current which is given by the following equations

$$I_{a-ratio} = \frac{I^k_{a-d1,\max}}{I_{a-d1,\max}} \quad , \quad I_{b-ratio} = \frac{I^k_{b-d1,\max}}{I_{b-d1,\max}} \quad , \quad I_{c-ratio} = \frac{I^k_{c-d1,\max}}{I_{c-d1,\max}} \tag{3.22}$$

Where

$I_{a-d1,\max}$, $I_{b-d1,\max}$, $I_{c-d1,\max}$ are the maximum peak value of wavelet of each phase

$I^{k}_{a-d1,\max}$, $I^{k}_{a-d1,\max}$, $I^{k}_{a-d1,\max}$ are the maximum peak value of kth sequence of wavelet form each phase (Youssef, 2002).

From equation 3.22, the suggested diagram is

If ($I_{a\text{-ratio}} > \varepsilon$ or $I_{b\text{-ratio}} > \varepsilon$ or $I_{c\text{-ratio}} > \varepsilon$) then

This is an inrush current

Else

This is an internal fault (Youssef, 2002).

### 3.4.3 Wave form analysis

Wave form analysis is a technique to distinguish between fault current and inrush current. This analysis is not able to identify transformer over excitation condition. There are two methods of discrimination between fault current and magnetizing inrush current, low current detection method and DC blocking method (Guzman, et al.,2004;IEEE, 2008a;Kasztenny&Kulidjian, 2000;Mekic, et al.,2006).

#### 3.4.3.1 Low current detection method

This method is based on the time intervals. Figure 3.12 shows the internal fault wave form and inrush current wave form using this method. According to this method, the differential current is compared with positive and negative thresholds. This threshold is the current close to zero and compares the time that wave form is below threshold values. If the time interval is less than a quarter cycle, it is internal fault. Versus, if the time interval is more than one quarter cycle, the wave form is inrush current (Guzman, et al., 2004;IEEE, 2008a;Kasztenny&Kulidjian, 2000).

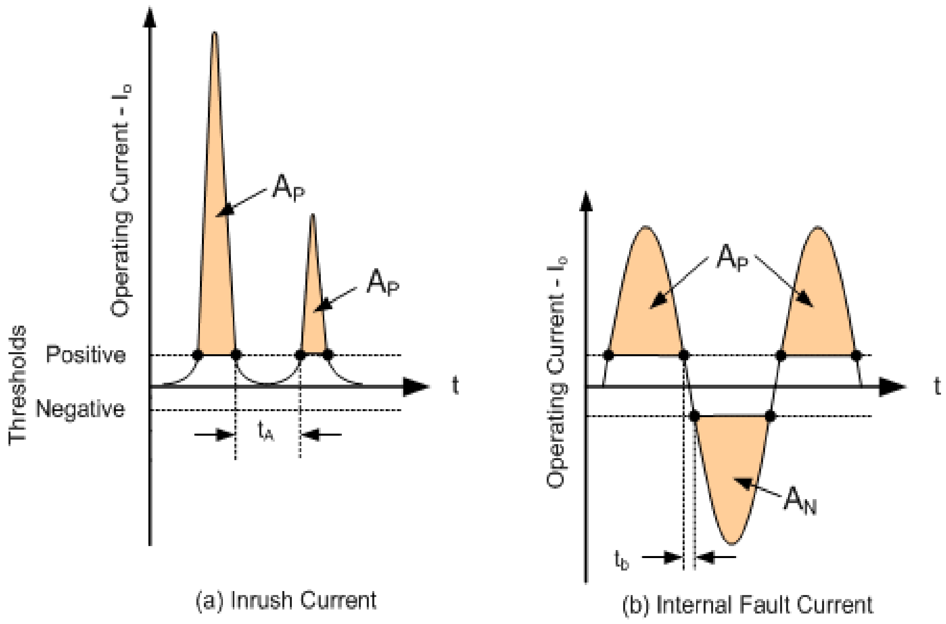


Figure 3.12: Low current detection inrush current (IEEE, 2008a).

#### 3.4.3.2 DC blocking method

This method depends on the DC offset. The DC component of inrush current is larger than the DC offset of internal fault. In this method, first, the positive wave shape and negative wave shape are extracted. In the new relays, this separation is very easy by using low pass filter. After the separation, the positive half cycle is proportional to the area $A_P$ and the negative half cycle is proportional to the area $A_N$. the summation positive $S_P$ and negative $S_N$ of one cycle are formed. The minimum and maximum absolute values of the two-one cycle are defined. To calculate the DC ratio, the smaller value is divided to the larger value. When $D_R$ (DC ratio) is less than threshold value it means that magnetization happens and the differential current is inrush current and operation of the relay should be restrained. Figure 3.13 shows the logic diagram for DC blocking method (Guzman, et al., 2004;IEEE, 2008a;Kasztenny&Kulidjian, 2000).

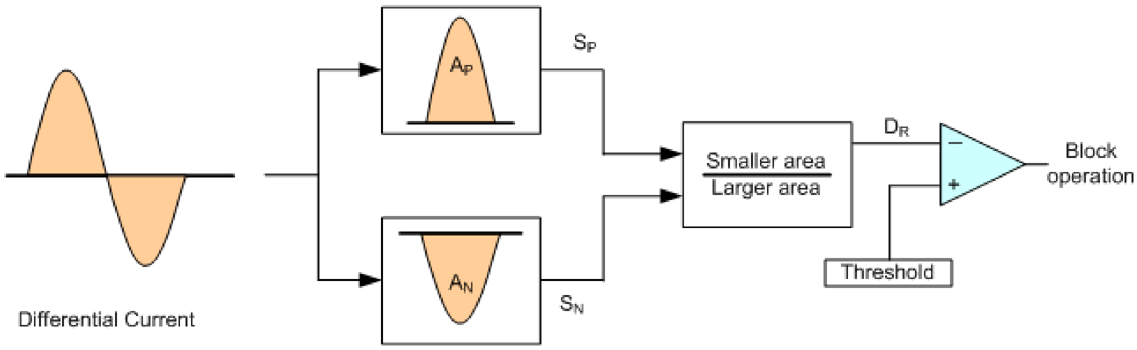


Figure 3.13: Logic diagram for DC blocking (IEEE, 2008a).

Another method to distinguish between inrush current and fault current is 2nd harmonic restraint or block which is common in numerical relays. This part will be discussed after the over excitation discussion.

## 3.5 Over excitation

The magnetic flux of transformer core is directly proportional to the supply voltage and inversely proportional to the frequency of the system. Over voltage or under frequency can produce flux in the transformer core that make transformer in saturation condition which causes thermal damage. Under frequency happens when generators of the system cut out or over load occurs at the system that generators cannot recover and feed all loads. Over voltage happens when the loads cut out the system or when a part of the system is separated because of disturbance (Guzman, et al., 2004; IEEE, 2008a; Nutt).

Consequences of over excitation are (Ebert, 2000):

1. Changing impedance and regulation
2. Changing load losses
3. Transformer makes noise
4. High short circuit
5. Shifting available Load Tap Changer range
6. Temperature rise.

### 3.5.1 Over excitation harmonic analysis

Fourier series is based on frequency analysis technique which is used for nonlinear systems. It is assumed that in the cause of sinusoidal excitation, approximately finite Fourier series can be used (Damnjanovic & Parsley; Huang, et al., 2002). From (Damnjanovic & Parsley), consider that:

$$\phi(t) = \phi_m \sin(\omega t) \tag{3.23}$$

The output current is periodic, thus

$$i(t) = \frac{A_0}{2} + \sum_{k=1}^{k=q} A_k \cos(k\omega t) + \sum_{k=1}^{k=q} B_k \sin(k\omega t) \tag{3.24}$$

$\frac{A_0}{2} = 0$ Where:

$$A_k = \frac{2}{T}\int_0^T i(t)\cos(k\omega t)d(\omega t), k = 1,2,3,...,q \tag{3.25}$$

$$B_k = \frac{2}{T}\int_0^T i(t)\sin(k\omega t)d(\omega t), k = 1,2,3,...,q \tag{3.26}$$

By using trigonometric identities, equation 3.24 change to

$$I_k = \sum_{k=1}^{k=q} (B_k + jA_k) \tag{3.27}$$

The gain of nonlinear system is

$$N_k(\phi_m, \omega) = \frac{B_k + jA_k}{\phi_m}, k = 1,2,3,...,q \tag{3.28}$$

If k=1, the fundamental wave is: $N_1(\phi_m, \omega) = \frac{B_1 + jA_1}{\phi_m}$ (3.29)

If k=q, the q-th harmonic component is

$$N_q(\phi_m,\omega) = \frac{B_q + jA_q}{\phi_m} \tag{3.30}$$

In the modern transformer the hysteresis loop is approximately by four slopes. It illustrates at figure 3.14.

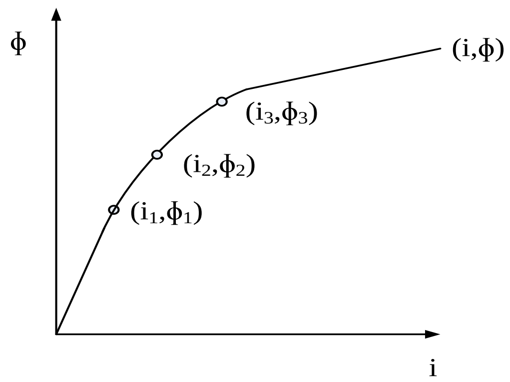


Figure 3.14: Approximation of the normalized magnetizing core (Damnjanovic & Parsley).

According to (Huang, Chung, Chen, & Chen, 2002), hysteresis loop, curve can be approximately assumed are lines with different slopes. Figure 3.14 is a result of this assumption. Figure 3.15 shows current in deferent part when hysteresis loop curve is approximated these lines and slopes.

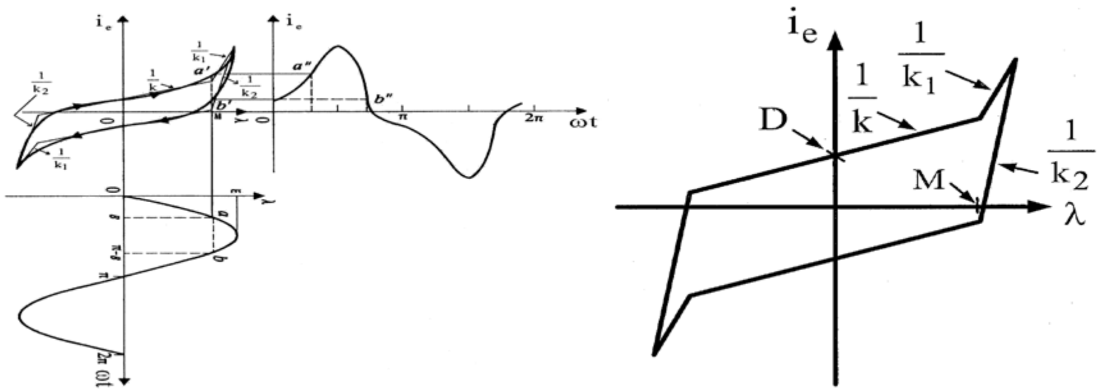


Figure 3.15: Approximated hysteresis loop to the lines (Huang, Chung, Chen, & Chen, 2002).

From figure 3.14 and 3.15 the approximation currents are:

$$i = (i_1 - m_1\phi_1) + m_1\phi \qquad \phi_0 < |\phi| \le \phi_1 \tag{3.31}$$

$$i = (i_2 - m_2\phi_2) + m_2\phi \qquad \phi_1 < |\phi| \le \phi_2 \tag{3.32}$$

$$i = (i_3 - m_3\phi_3) + m_3\phi \qquad \phi_2 < |\phi| \le \phi_3 \tag{3.33}$$

$$i = (i_4 - m_4\phi_4) + m_4\phi \qquad \phi_3 < |\phi| \le \phi_4 \tag{3.34}$$

Where

$$i = \phi_m \sin(\omega t) \tag{3.35}$$

Thus

$$i = (i_k - m_k\phi_k) + m_k\phi \qquad \phi_{k-1} < |\phi| \le \phi_k \qquad k = 1,2,3,...,q \tag{3.36}$$

If h=2k+1, k=0,1,2,3,…,q and $ab\cos(\omega t)$ is core losses part, real part and imaginary part of current are:

At first for fundamental component, k=0 and h=1

$$R_{e1} = \frac{4}{\pi\phi_m}\sum_{n=1}^{p}(i_n - m_n\phi_n)(\cos\alpha_{n-1} - \cos\alpha_n) + \frac{4}{\pi\phi_m}\sum_{n=1}^{p}(\frac{\alpha_n}{2} - \frac{\alpha_{n-1}}{2} + \sin 2\alpha_{n-1} - \sin 2\alpha_n) \tag{3.37}$$

And for other harmonic components

$$R_{ek} = \frac{4}{\pi\phi_m}\sum_{n=1}^{p}\frac{1}{2k+1}(i_n - m_n\phi_n)[\cos(2k+1)\alpha_{n-1} - \cos(2k+1)\alpha_n] +$$

$$\frac{1}{\pi}\sum_{n=1}^{p} m_n[(\sin 2k\alpha_n - \sin 2k\alpha_{n-1}) + \frac{1}{k+1}(\sin(2k+1)\alpha_{n-1} - \sin(2k+1)\alpha_n] \tag{3.38}$$

Where

$$\alpha_1 = \sin^{-1}(\frac{\phi_1}{\phi_m}),...,\alpha_4 = \sin^{-1}(\frac{\phi_4}{\phi_m})$$

In the imaginary part, in fundamental component imaginary part equals to maximum of core losses (ab) and for the other harmonic components, imaginary parts are zero (Damnjanovic & Parsley).

Because the excitation current is an odd function, thus in the period of T/2 the Fourier series contains odd components. Hence the over excitation current contains odd harmonics components (Damnjanovic & Parsley).

## 3.6 Harmonic restraint and blocking

The common method to distinguish between fault and conditions which are the same as fault (magnetizing inrush current or over excitation) for REF relay is harmonic restraint and blocking. The following discussions are presented:

### 3.6.1 Harmonic restraint

One way of distinguishing between fault and phenomena which cause mal-operation is harmonic restraining. There are different methods to restrain harmonics (IEEE, 2008a).

Single phase transformer, the limitation setting for the restraining relay at $2^{nd}$ harmonic is 20% of nominal current and for limit of $5^{th}$ harmonic restraining current is 35% of nominal current (C.H.Einvall & J.R.Linders, 1975; Guzman, et al., 2004).

Figure 3.16 shows the simple differential or REF relay with restraint and operation circuits. Filters in this circuit are the main parts of this simple circuit. This figure shows two filters. The first filter that is in the operation part is series resonance filter. This filter has resonance at the fundamental frequency, it has low impedance, thus the operation coil only energizes at the fundamental frequency when the current is more than pick up current. From the other point of view, the parallel L and C is a resonance filter. When current has large harmonic component, this filter passes the harmonics part, therefore it energizes the restraint coil. Thus at the conditions that harmonics are produced (magnetizing inrush or over excitation) and the harmonic components are more than setting, this part restrains the false operation of the relay.

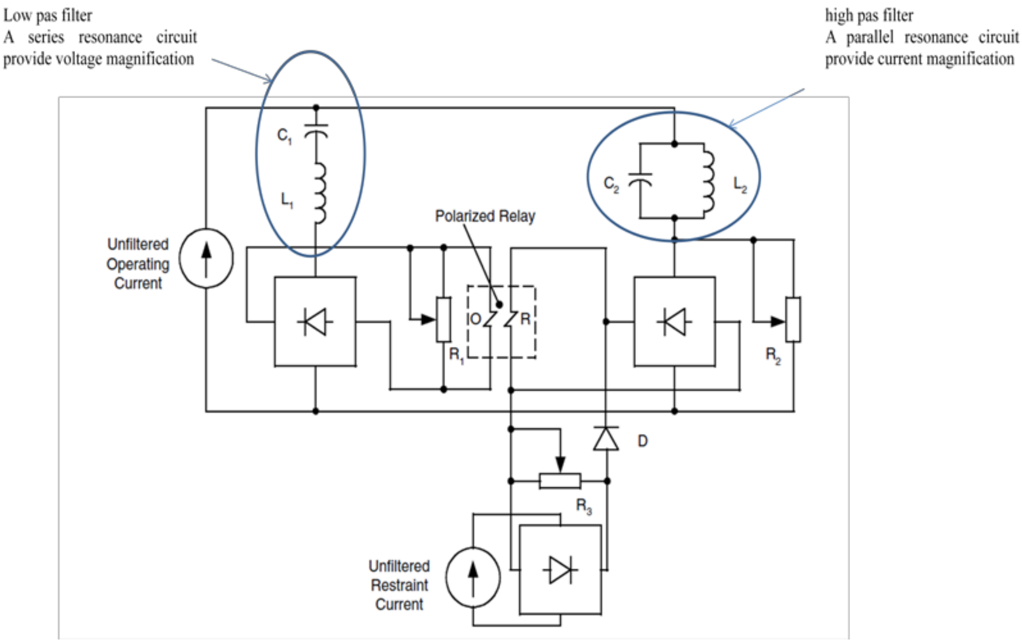


Figure 3.16: Differential relay with restraint and operation circuit (Guzman, J.Alture, & Benmonyal, 2004).

Assume there is a tow winding transformer, the restraint current is vectorial summation of two input of the REF relay (residual current and star point current). Thus (Guzman, et al., 2004; IEEE, 2008a)

$$I_{RT} = k(|\bar{I}_{w1}| + |\bar{I}_{w2}|) \tag{3.39}$$

Where, k is a constant. Then, the operation current is

$$I_{op} > SLP.I_{RT} + k_2 I_2 + k_3 I_3 + ... \tag{3.40}$$

Where, SLP is the slope of relay characteristic. By connection inside current transformer of relay, the 3rd harmonic can be bypassed and it is assumed that inrush current has a large 2nd harmonic and other even harmonics are neglected. Also over excitation has 5th harmonic and other odd harmonics are neglected, thus the operation current is

$$I_{op} > SLP.I_{RT} + k_2 I_2 + k_5 I_5 \tag{3.41}$$

And if the transformer is three phase transformer, equation 3.41 change to

$$I_{op} > SLP.I_{RT} + \sum_{n=1}^{3}(k_2 I_2 + k_5 I_5) \tag{3.42}$$

Figure 3.17 shows the logic diagram of a simple equation of 3.41. This figure illustrates how the restraint diagram works, also, the way that all components are compared together to produce trip signal. At figure 3.17, this circuit produces restraint harmonic only on 5th harmonic. However 2nd harmonic (magnetizing inrush current) needs harmonic blocking circuit.

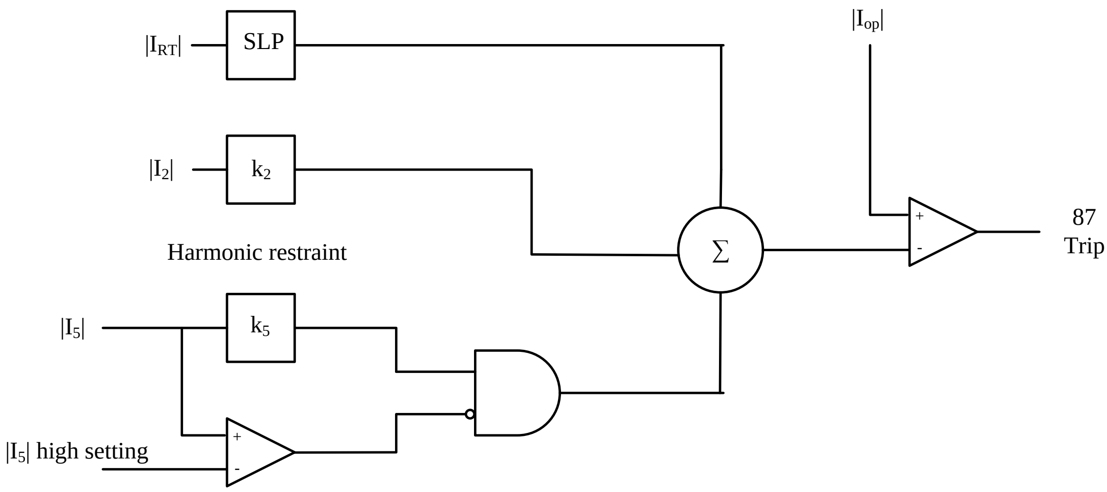


Figure 3.17: Second and fifth harmonic restraint logic circuit (IEEE, 2008a).

### 3.6.2 Harmonic blocking

This method is the same as harmonic restraining. It is used for distinction between fault and magnetizing inrush current (Guzman, et al., 2004; IEEE, 2008a). This method at first was proposed by R. L. Sharp and W. E. Glassburn ("A transformer differential relay with second-harmonic restraint", *AIEE trans., 913,918*). In this section, Differential Unit (DU) and Harmonic Blocking Unit (HBU) is identified (Guzman, et al., 2004; IEEE, 2008a).

Figure 3.18 shows a simple differential unit. In this unit, in the side of operation, according to $I_{op} = \left|\vec{I}_{w1} + \vec{I}_{w2}\right|$, the current first is rectified and it is applied to the operation coils. At the restraint part, air gap auxiliary current transformer makes proportional voltages and rectifies the both voltages and chooses the maximum voltage magnitude. Then, restraint current is produced and it is applied to the restraint coil. In this figure $R_1$ is used to determine the relay slope of operation characteristic of relay (Guzman, J.Alture, & Benmonyal, 2004).

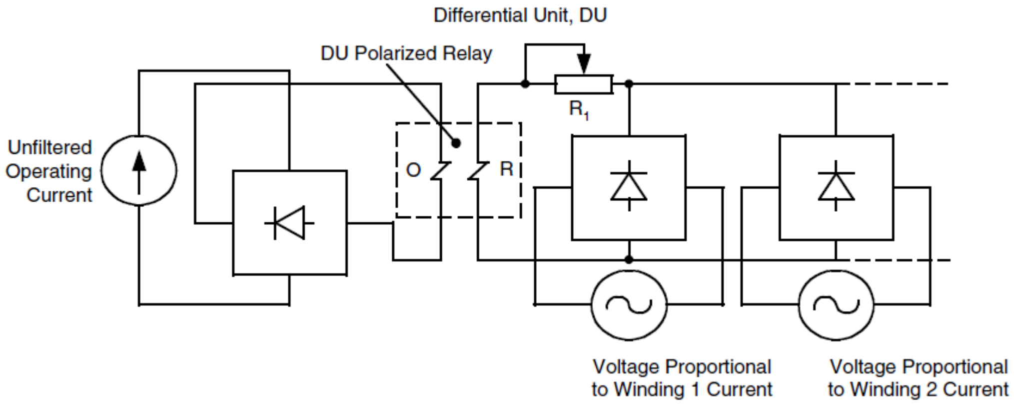


Figure 3.18: Differential unit (Guzman, J.Alture, & Benmonyal, 2004).

At harmonic blocking unit, relay has air gap auxiliary current transformer which omits the DC component at inrush current. Figure 3.19 shows the HBU. As it illustrates, at the operation part, there is a parallel L, C resonance filter which is tuned at two times fundamental frequency. It means at the second harmonic the impedance is maximum and the other component is passed from this filter. Thus operating current contains fundamental component, 3rd harmonic, 4th harmonic and etc. On the restraint section, there is a parallel L and C that are series with L which is tuned at fundamental frequency. It means this filter has maximum impedance at fundamental frequency (IEEE, 2008a). Thus, the operating condition is

$$I_{op} + k_3 I_3 + k_4 I_4 + \ldots > k_2 I_2 \quad (3.43)$$

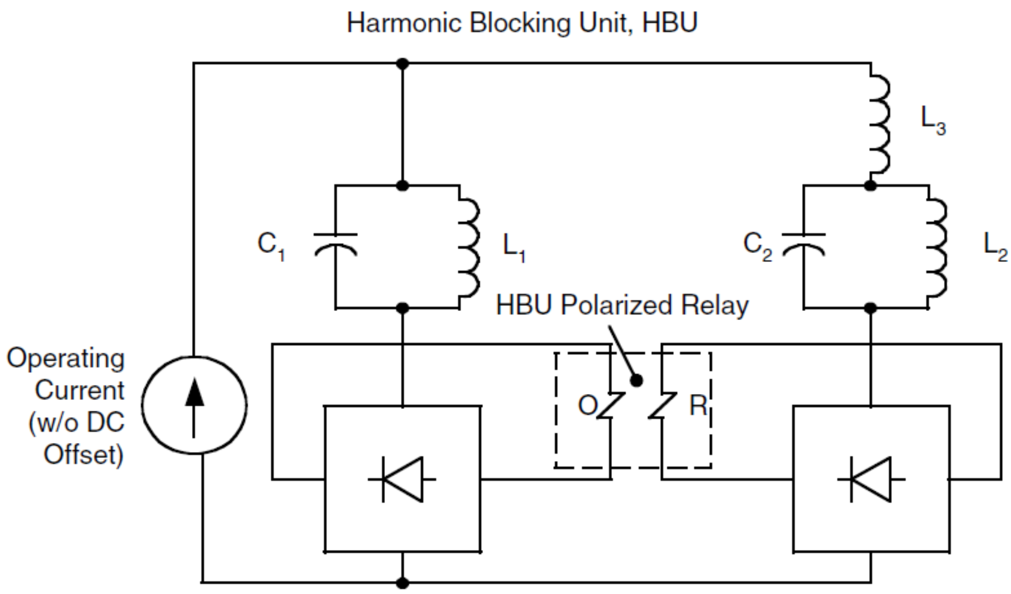


Figure 3.19: Harmonic block unit (Guzman, J.Alture, & Benmonyal, 2004).

Figure 3.20 shows the relay contacts. T is a timer for response of the filters. 86 is a lock out relay. The relay also include the instantaneous over current relay for sever fault current (Guzman, J.Alture, & Benmonyal, 2004).

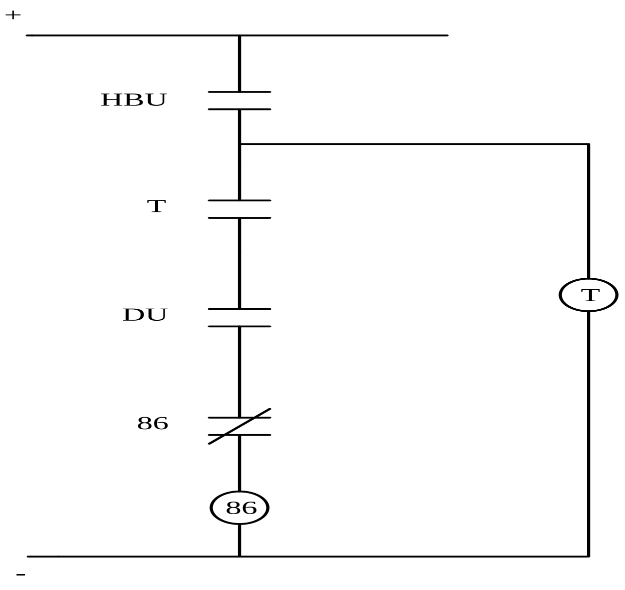


Figure 3.20: Transformer relay second harmonic contact (Guzman, J.Alture, & Benmonyal, 2004).

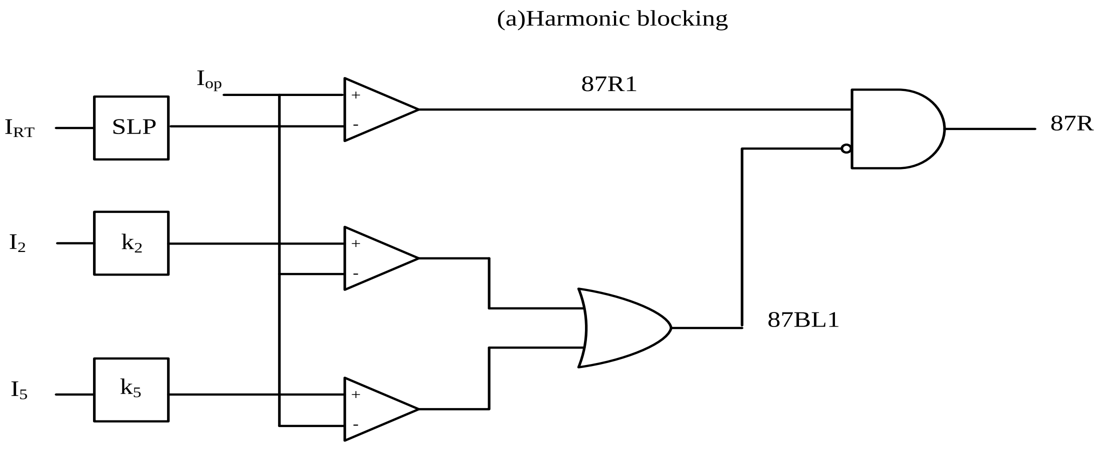


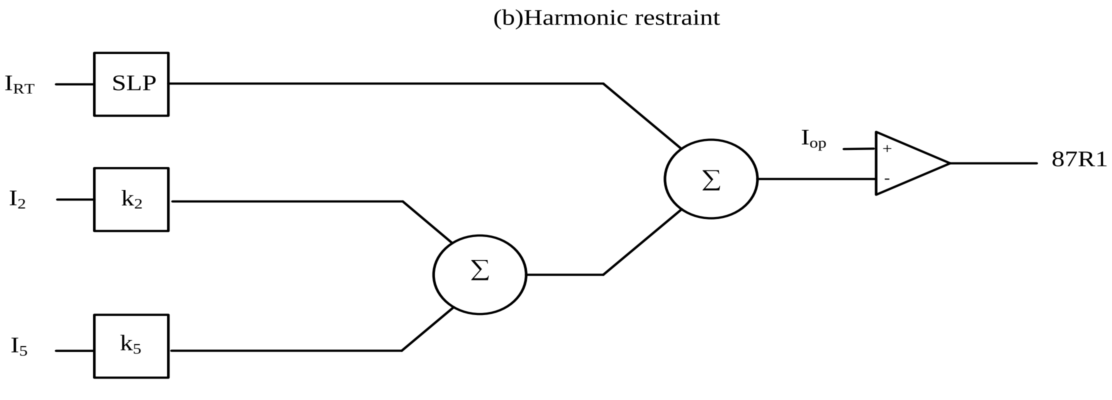


Figure 3.21: Harmonic blocking and restraint logic diagram (Guzman, J.Alture, & Benmonyal, 2004).

Figure 3.21 shows the logic diagram of harmonic blocking scheme and harmonic restraint scheme. Part b at this figure is the logic diagram of equation 3.41. But part a, shows if magnetizing inrush current or core over excitation occurs or both of them occur, the relay does not work. Otherwise the relay operates by operation current. Also at harmonic restraining, $I_{RT}$ combines with the harmonic component and then is compared with the $I_{op}$, but in the harmonic blocking $I_{RT}$ only is used at comparison level.

There are two different kinds of harmonic restraints that is used in REF for three phase transformer (differential relay), independent harmonic restraint and independent harmonic blocking (Guzman, J.Alture, & Benmonyal, 2004). According to the below figure, if relay has blocking diagram and it does not work and relay restraint circuit works, relay has restraint signal.

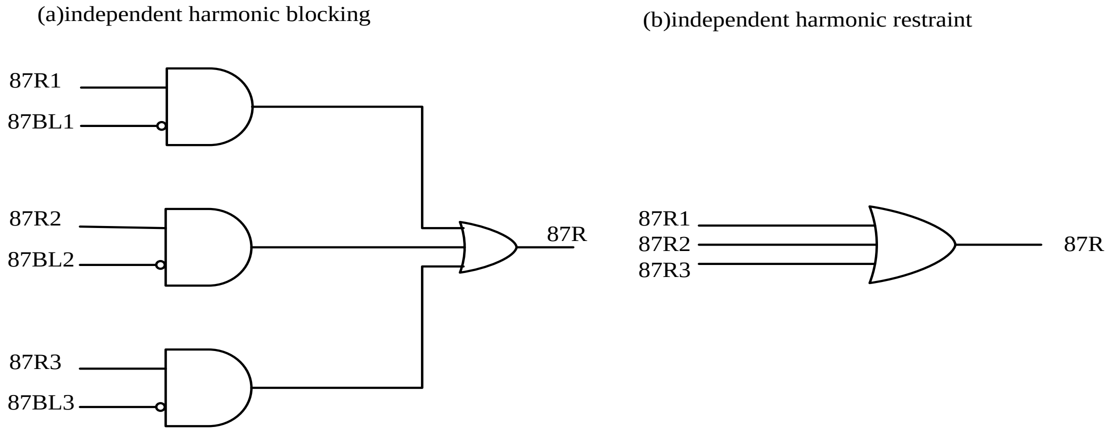


Figure 3.22: Independent harmonic blocking and restraint (Guzman, J.Alture, & Benmonyal, 2004).

New numerical REF (differential) relays are flexible to choose even harmonic restraint or blocking for inrush current, the fifth harmonic and dc blocking [1]. It comes back to the network topology, according which topology the designer can choose blocking or restraint circuit. New numerical relays (like Siemens) have a CFC table that can be chosen.

Table 3.1 compares blocking and restraint scheme. According to the table 3.1, at any condition which causes mal-operation, the best scheme on the certain network topology can be chosen.

Table 3.1: Comparing between harmonic restraint and blocking (Guzman, J.Alture, & Benmonyal, 2004).

| | All-harmonic restraint(HR) | Harmonic blocking(HB) |
|---|---|---|
| Security of external fault | Higher | Lower |
| Security of inrush current | Higher | Lower |
| Security of overexcitation | Higher | Lower |
| Dependability | Lower | Higher |
| Speed | Lower | Higher |
| Slope characteristic | Harmonic dependent | well |
| Testing | Result depend on harmonic | simple |

According to the discussions in this chapter, now the investigation about each algorithms that are mentioned in chapter two. At the beginning, GE new algorithm is studied.

## 3.7 General Electric Multilin

This algorithm should be avoided from mal-operation at magnetizing inrush current, over excitation condition and sever CT saturation. When an external fault occurred and cleared, the differential current and restraint current are decaying, thus the diagram should be worked at restraint area which means uncontrolled decaying may go to the operation zone and causes false operation of the REF relay (Kasztenny & Kulidjian, 2000; Kasztenny, et al., 2004). Figure 3.23 shows the uncontrolled and controlled external fault clearing.

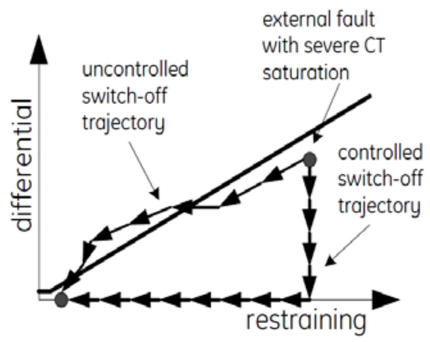


Figure 3.23: Operation during clearing fault (Kasztenny, 2000; Kasztenny, et al., 2004).

According to equation 2.32, if the positive sequence of current is less than 1.5 times of nominal phase current, for maximizing sensitivity on low current internal fault the positive restraint current equal to $1/8^{th}$ positive sequence. On the other point, the positive sequence is more than 1.5 times of nominal phase current, if the positive sequence is more than zero sequence, it means ground fault current is very low, thus for the positive restraint current equals to three times of difference between positive sequence and zero sequence. The zero sequence current reduces the restraint and increases the sensitivity of relay on high current internal fault.

Equation 2.33 shows the formula for making negative restraint component. It shows that normally three multiplier is used but at the certain conditions such as energizing inrush current the one multiplier is used and time delay function (see figure 2.27).

Multipliers 1/8th at positive sequence or one at negative sequence of restraint signal is used because at the transient component may occur spurious components (Kasztenny, Sharples, Campbell, & Pozzuoli).

There are two methods to determine the symmetrical components

- *Phasor estimator plus phase shifter* first it estimates the phasors of phase signals and then it calculates the symmetrical components
- *Phase shifter plus phase estimator* first, approach shifts the phase signals in time domain and then estimates the phasors.

These two ways of determining the symmetrical components which is used in the GE diagram are linear operations. Thus, numerical relay with signal processing can work.

According to equation 2.34, the significant restraint at CT saturation condition following initial states before saturation is produced. While the fault current decays, the restraint signal increases even if the CT saturation produces the lower restraint current (because of exponentially decaying) (Kasztenny, 2000; Kasztenny, et al., 2004).

Also this algorithm is a unique algorithm that uses symmetrical components to make restraint signal. In the following, the typical simulation on this algorithm which is proposed by GE at (Kasztenny & Kulidjian, 2000; Kasztenny, et al., 2004) is assessed. If at the typical network external double line to ground happened, figure 3.24 from (Kasztenny & Kulidjian, 2000)shows the phases and ground currents.

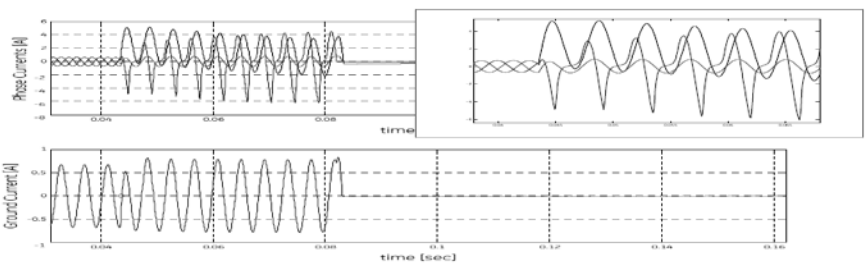

Figure 3.24: Phases and ground currents of external double line to ground fault (Kasztenny & Kulidjian, 2000).

Symmetrical component of this network at external double line to ground is shown in figure 3.25. It illustrates, positive sequence has largest magnitude from fault beginning time until clearing  and zero sequence and negative sequence have large magnitude respectively after positive sequence (according to the double line fault calculation) .

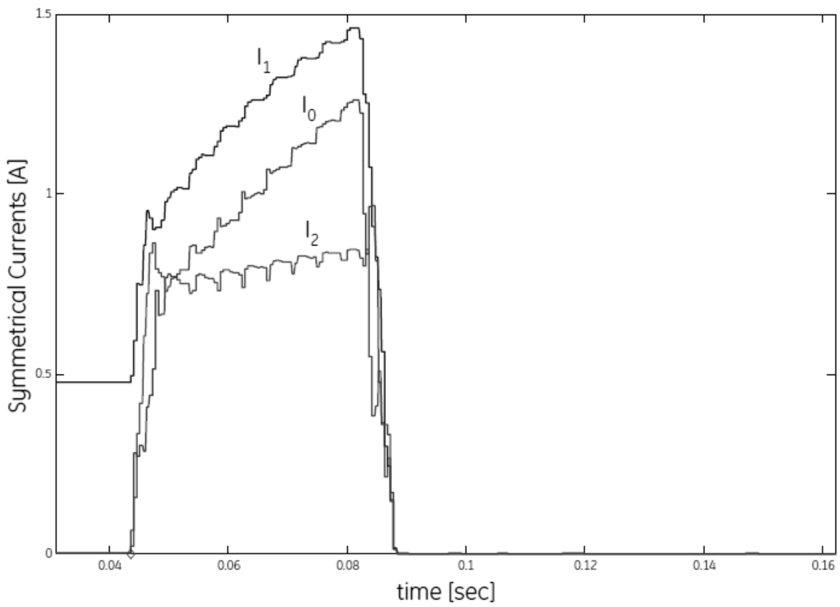


Figure 3.25: Symmetrical component of external double line to ground (Kasztenny & Kulidjian, 2000).

Figure 3.26 shows the restraint symmetrical components according to the symmetrical components of double line to ground fault that is illustrated in figure 3.25. It is shown that the largest component is zero sequence of restraint current. Also at the next curve of this figure, the total restraint current is shown. Also it is illustrated the exponentially decaying equation 2.34. It illustrates at around 0.08 sec, when the fault is cleared, the curve decreases continual.

Next figure, figure 3.27 shows the differential current that is obtained according to the equation 2.29 and total restraint current. This figure illustrates in the external fault REF relay must not operate, thus according to this simulation, the relay did not operate. As this figure illustrates, the restraint current is greater than the differential current.

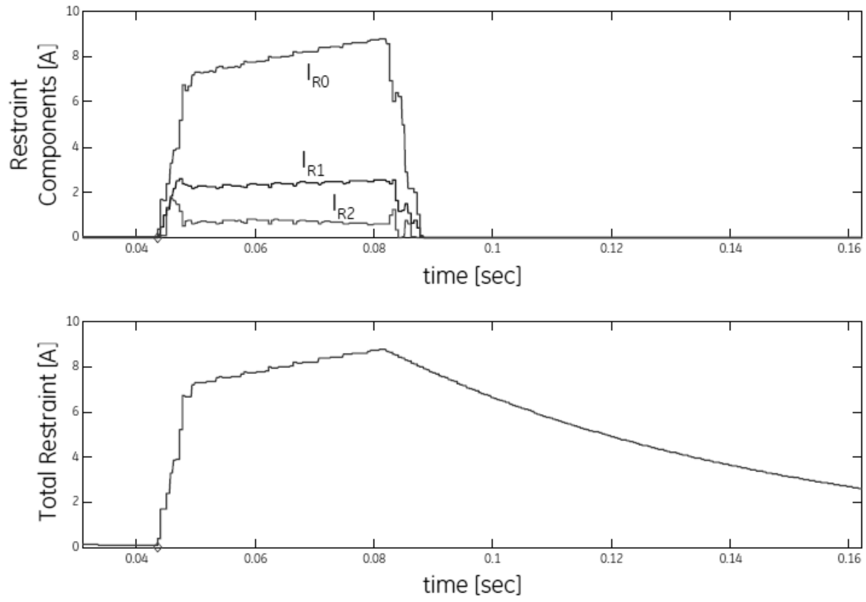


Figure 3.26: External double line to ground fault restraint component and total (Kasztenny & Kulidjian, 2000).

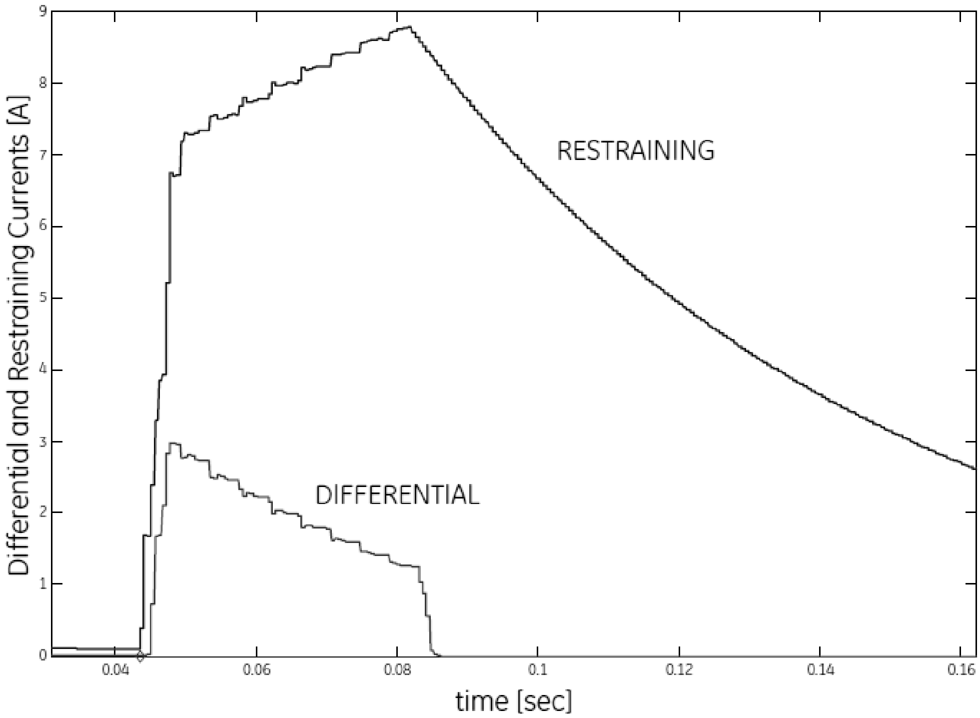


Figure 3.27: External double line to ground fault restraint and differential currents (Kasztenny & Kulidjian, 2000).

Figure 3.28 shows the condition at switching operation for this typicaly fault. This figure illustrates when the external double line to ground fault happens and CT goes to saturation area. After fault is cleard and this diagram deacreses the restricted earth fault by control without any mal-operation instead reduction of fault current.

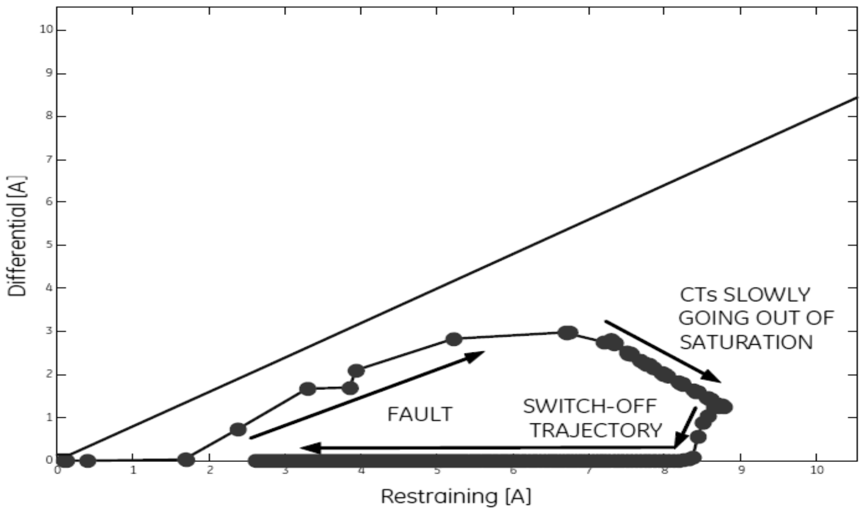


Figure 3.28: Relay characteristic at external double line to ground and clearing (Kasztenny & Kulidjian, 2000).

The following simple case study for GE algorithm is at steady state condition. Assumed all currents are in per unit. First, it is assumed that a single line to ground fault occurs at the external protection zone, thus according to (Grainger & Stevenson, 1994; Hadi, 2007), equation 2.16 and figure 2.8 become:

$I_A = 1.0\angle 0°$ , $I_B = 0, I_C = 0$

$I_G = 1.0\angle 180°$

$I_0 = I_1 = I_2 = \frac{I_A}{3} = 0.33\angle 0°$ , thus

$I_{R1} = \frac{1}{8}.0.33 = 0.04125$ , $I_{R2} = 3.0.33 = 0.99$ , $I_{R0} = |I_G - I_N| = |1.0\angle 180 - 1.0\angle 0| = 2$

Therefore, $I_R = 2$

$$I_D = \left|I_G + I_N\right| = \left|1.0\angle 180 + 1.0\angle 0\right| = 0$$

Hence, the relay does not operate and it goes to restraint area. Now, inside the protection zone, fault is calculated again. The fault is single line to ground and the phase currents are exactly the same as previous calculation. Thus

$$I_A = 1.0\angle 180^\circ,\ I_B = 0, I_C = 0$$

$$I_G = 1.0\angle 180^\circ$$

$$I_0 = I_1 = I_2 = \frac{I_A}{3} = 0.33\angle 180^\circ$$ , thus

$$I_{R1} = \frac{1}{8}.0.33 = 0.04125,\ I_{R2} = 3.0.33 = 0.99,\ I_{R0} = \left|I_G - I_N\right| = \left|1.0\angle 180 - 1.0\angle 180\right| = 0$$

Therefore, $I_R = 0.99$

$$I_D = \left|I_G + I_N\right| = \left|1.0\angle 180 + 1.0\angle 180\right| = 2$$

According to the values of the restraint current and differential current, relay operate instead of fault occurred inside of protection zone.

This algorithm has good security instead of magnetizing inrush current, over excitation and CT saturation. This algorithm is a unique REF protection algorithm which uses symmetrical components to produces restraint signal. Also, according of sever external earth fault that may cause internal earth fault this algorithm has good security. This algorithm does not need complicated filters for defining certain conditions like magnetizing inrush. But some conditions produce spurious zero and negative components that cause mal-operation. Because this algorithm based on symmetrical component, for sensitivity and security extra algorithm for filtering this spurious components and distinguishing between fault and false condition is needed.

## 3.8 Siemens algorithm

According to equation 2.26, $I_{REF}$ is derived from fundamental wave and this current produces the tripping signal in Siemens algorithm [2]. In the following, equations 2.26 and 2.27 are clarified by three conditions. Assume that k = 1:

- *An external fault current*, according to the figure 2.23, $3I_0$” and $3I_0$’ have equal magnitude with opposite direction, thus

  $$3\bar{I}_0'' = -3\bar{I}_0'$$

  $$I_{REF} = |3I_0'|$$

  $$I_{REST} = |3\bar{I}_0' + 3\bar{I}_0''| - |3\bar{I}_0' - 3\bar{I}_0''| = 2.|3\bar{I}_0'|$$

  This calculation illustrates that the tripping current is equal to star point current and restraint current equals to twice of star point current. Therefore the relay does not operate.

- *An internal earth fault which is fed only from the star point*, in this case the residual current is zero, $3I_0$”=0. Then

  $$I_{REF} = |3I_0'|$$

  $$I_{REST} = |3\bar{I}_0' - 0| - |3\bar{I}_0' + 0| = 0$$

  Calculation shows that full sensitivity during an internal earth fault. When the earth fault occurs inside the protection zone because of the tripping signal coming from star point, the relay operates.

- *Internal earth fault which is fed from the system and star point*, in this case assuming the residual current and star point current have the same magnitude, results to

  $3\bar{I}_0'' = 3\bar{I}_0'$

  $I_{REF} = |3I_0'|$

  $I_{REST} = |3\bar{I}_0' - 3\bar{I}_0'| - |3\bar{I}_0' + 3\bar{I}_0'| = -2.|3\bar{I}_0'|$

  The tripping element, $I_{REF}$ equals to star point current and restraint current is twice of star point current and negative, therefore it is set to zero (Siemens).

Above calculations in different conditions show that the sensitivity of this relay is high. These calculation shows at internal earth fault the restraint current is zero or negative but external earth fault produces large restraint current.

Figure 3.29 shows when the residual current is high, the restraint current goes high too. The vertical axis of this graph is ratio of earth currents ($3I''_0/3I'_0$). Assume the ideal current transformer at external earth fault $3I''_0/3I'_0$ equals to -1. This figure shows that tripping in restricted earth fault depends on earth currents ratio ($3I''_0/3I'_0$); Where $I_{REF}>$ is the setting value.

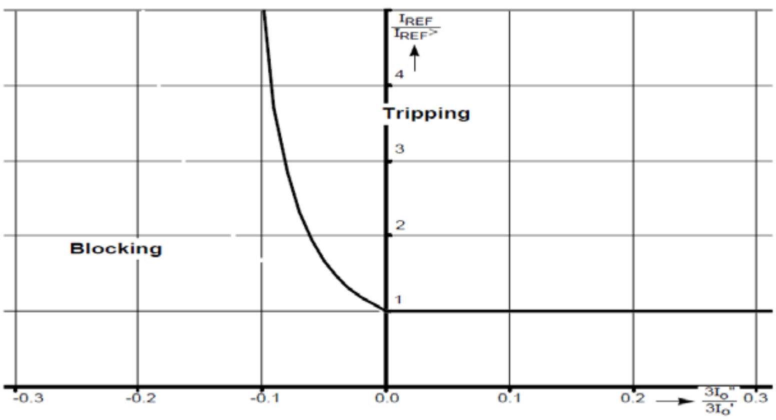


Figure 3.29: Tripping area depends on earth currents ratio (Siemens).

According to the equations 2.24 and 2.27, $I_{op} = |3I'_0|$

For $-90° \le \varphi(3I'_0 : 3I''_0) \le +90°$, thus the relay operates if $I_{op} \ge I_{REST}$

And in the expanded area

$$I_{op} = 3I'_0 - k_0 I_{REST}$$

For $+90° \le \varphi(3I''_0 : 3I'_0) \le +270°$, thus the relay operates if $I_{op} \ge I_{REST}$ (G.Ziegler, 2008).

CT saturation can change the phase displacement between the residual current and star point current. This phase shifting can reduce the restraint current and this event cause mal-operation of relay. If the phase displacement is $\varphi(3I''_0 : 3I'_0) = 90°$, then the restraint current is zero. For instance,

$$3I'_0 = 1\angle 0°, 3I''_0 = 1\angle 90°$$

$$I_{REST} = k.(|3\bar{I}_0' - 3\bar{I}_0''| - |3\bar{I}_0' + 3\bar{I}_0''|)$$

$$I_{REST} = k.(|1\angle 0° - 1\angle 90°| - |1\angle 0° + 1\angle 90°|) = k(1.4142 - 1.4142) = 0$$

This phase shifting also can cause the relay to operate at external earth fault. Figure 3.30 shows the vectorial summation of residual current and star point current that result in making restraint current. As this figure illustrates, phase displacement between residual current and star point current vector, because of CT saturation, the restraint current is less than the tripping effect, therefore the relay operates.

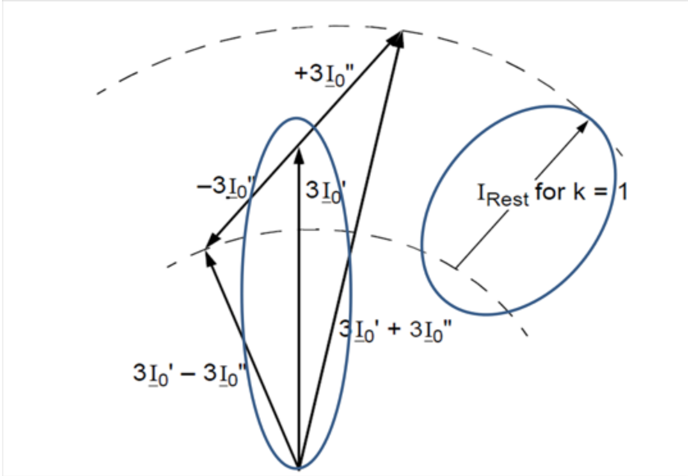


Figure 3.30: Phasor diagram during external fault (Siemens).

Another factor that influences the restraint current is k or stabilization factor. Stabilization factor has relation to the angle limitation $\phi_{limit}$. Figure 3.31 shows this relationship. This graph shows the angle and value of $I_{REF}/I_{REF}>$ the relay goes to operation or blocking area. For instance, in 7UT6 k=4 the restraint values for the external earth fault is 8 times of tripping effect current $I_{REF}$ and the limit angle is 100° which means there is no trip if the angle between residual current and star point current is more than 100°.

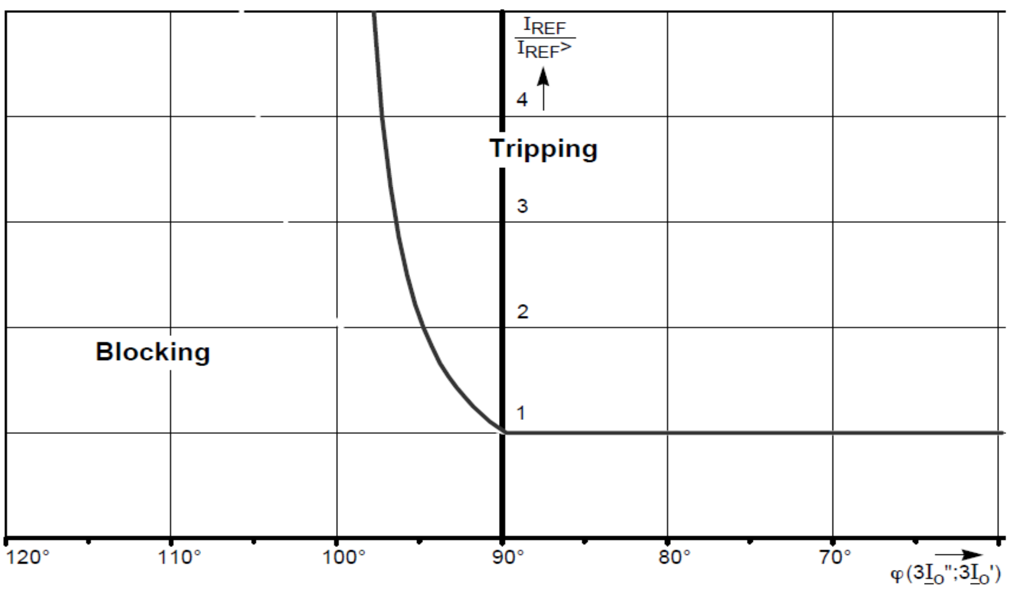


Figure 3.31: Tripping characteristic by phase limit (Siemens).

K factor can be changed, thus regarding to the change of k, the limit angle changes. The limit angle is between zero degree for internal fault and 180 degree for external fault. Table below shows the limitation angle regarding to different k factor.

Table 3.2: k factor and limit angle (G.Ziegler, 2008).

| k factor | $\varphi_{\lim it}$ |
|---|---|
| 1.0 | 130 |
| 1.4 | 120 |
| 2.0 | 110 |
| 4.0 | 100 |
| ∞ | 90 |

Also figure 3.32 shows the relation between k and limit angle in a polar plane. In this graph assume $\frac{3I''_0}{3I'_0}=1$ and the phase displacement between mentioned vector that the magnitude equals to one, the angle equals to zero and vector of $\frac{3I'_0}{3I''_0}.e^{\varphi(3I'_0/3I''_0)}$ . For instance, for k=4, the tripping area is between 260 and 100 degree.

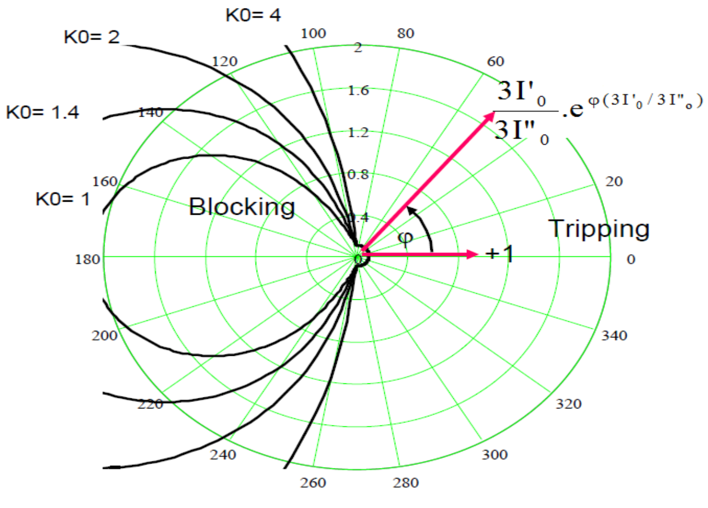


Figure 3.32: Polar characteristic show (G.Ziegler, 2008).

Figure 3.33 shows the simple logic diagram of REF relay operation. This relay has the ability to turn off REF function or turn on or goes to blocking mode. The option of blocking means that relay operates but the tripping signal is blocked. Block section of logic diagram shows if the relay is not blocking and switch 1 is "on" condition, the relay can operate. Thus if current value is more than pick up value and slope function (1313) REF states, function of 1312 relay operates after time delay.

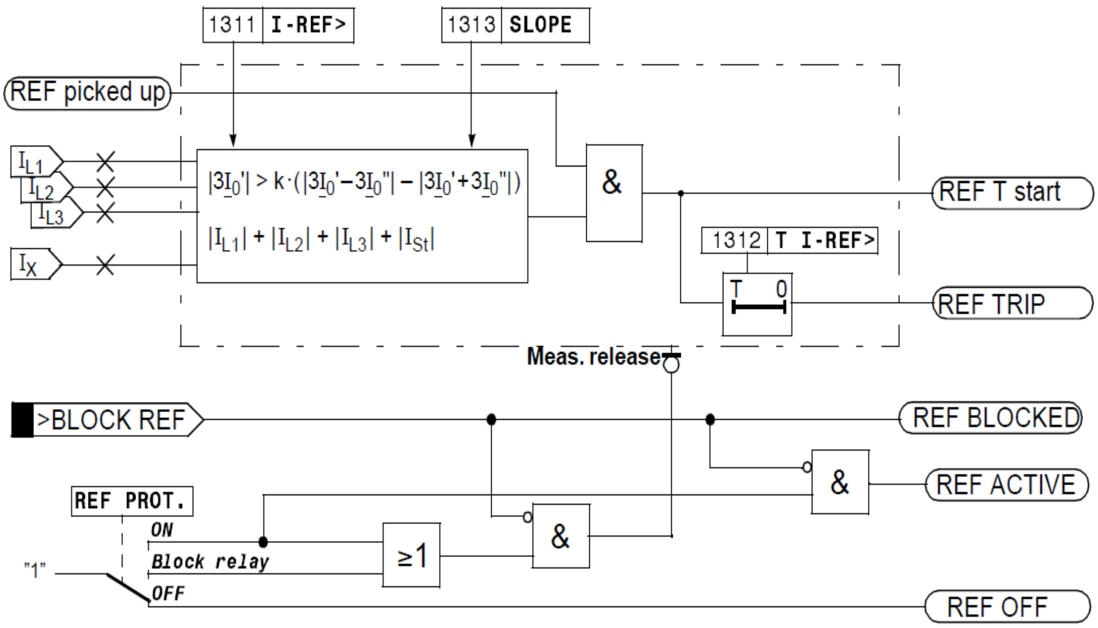


Figure 3.33: Simple logic diagram of the REF (Siemens).

Figure 3.34 illustrates the REF relay characteristic. IDIFF> is the pickup current value which is set by the user. For appropriate good sensitivity and security, this relay has 2 slopes. Also there is a certain region for high short circuit current that the slope is low proportional to the other slopes.

This relay uses separate filters for magnetizing inrush current and over excitation. It has a good flexibility with regard to the network and users can set the relay based on a certain network. The security of this relay is high because many slope and all part calculate separately is used. The disadvantage of this relay is using time delay for tripping that may cause many damages. This time delay is used for calculation of condition of fault that has been sensed and this delay is except of inherit time delay of each process step. It causes the speed problem in the relay. But, because of operation of this relay is based on vectorial summation of currents, the security of operation of this relay is very high.

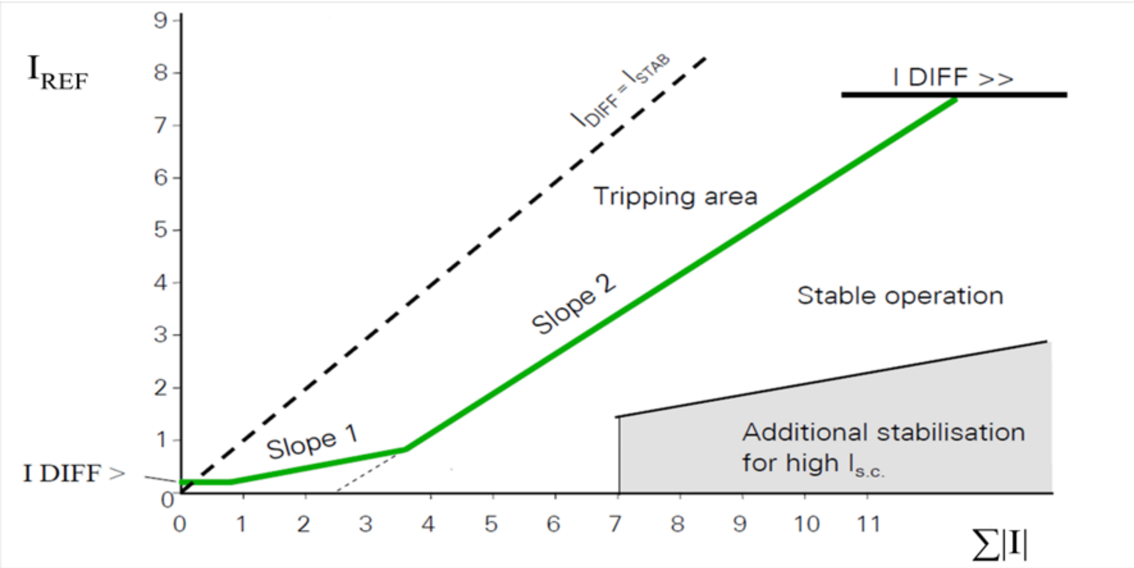


Figure 3.34: Siemens REF characteristic curve (G.Ziegler, 2008; Siemens).

## 3.9 ABB algorithm

This relay like Siemens relay works on vectorial comparison. According to the figure 2.32, for external earth fault, assume that the both CTs (residual and star point) are same. As this figure illustrates, $I_N$ and $3I_0$ have equal magnitudes with phase displacement of 180 degree. For internal earth fault, figure 2.33 shows there are two way for circulating current. The current comes from neutral point and another comes from system. In this case $I_N$ and $3I_0$ are almost with the same direction. As been mentioned in chapter two, this relay work on fundamental zero sequence, thus these currents are fundamental frequency of zero sequence. According to these assessments, if Relay Operating Angle (ROA) becomes smaller, the REF can be stabled under sever external faults (ABB).

Table 3.3 shows the data of operating REF relay.

Table 3.3: Data of bias characteristic of REF in ABB relay (ABB).

| Default sensitivity $I_{dmin}$ (zone1) | Max.base sensitivity $I_{dmin}$ (zone1) | min.base sensitivity $I_{dmin}$ (zone1) | End of zone 1 | First slope | Second slope |
|---|---|---|---|---|---|
| %Irated | %Irated | %Irated | %Irated | % | % |
| 30 | 4 | 100 | 125 | 70 | 100 |

Figure 3.35 shows the relay characteristic. This figure illustrates the different sensitivity of this relay that users can configure. Also it reveals that this relay is dual slope. Slope 1 is in zone 1 and slope 2 is in zone 2. Bias current from 0 till 1.25 p.u determines the zone 1and 1.25 till 2.5 determines zone 2. This curve illustrates the operate area and block area and according to chosen sensitivity, these zone areas change.

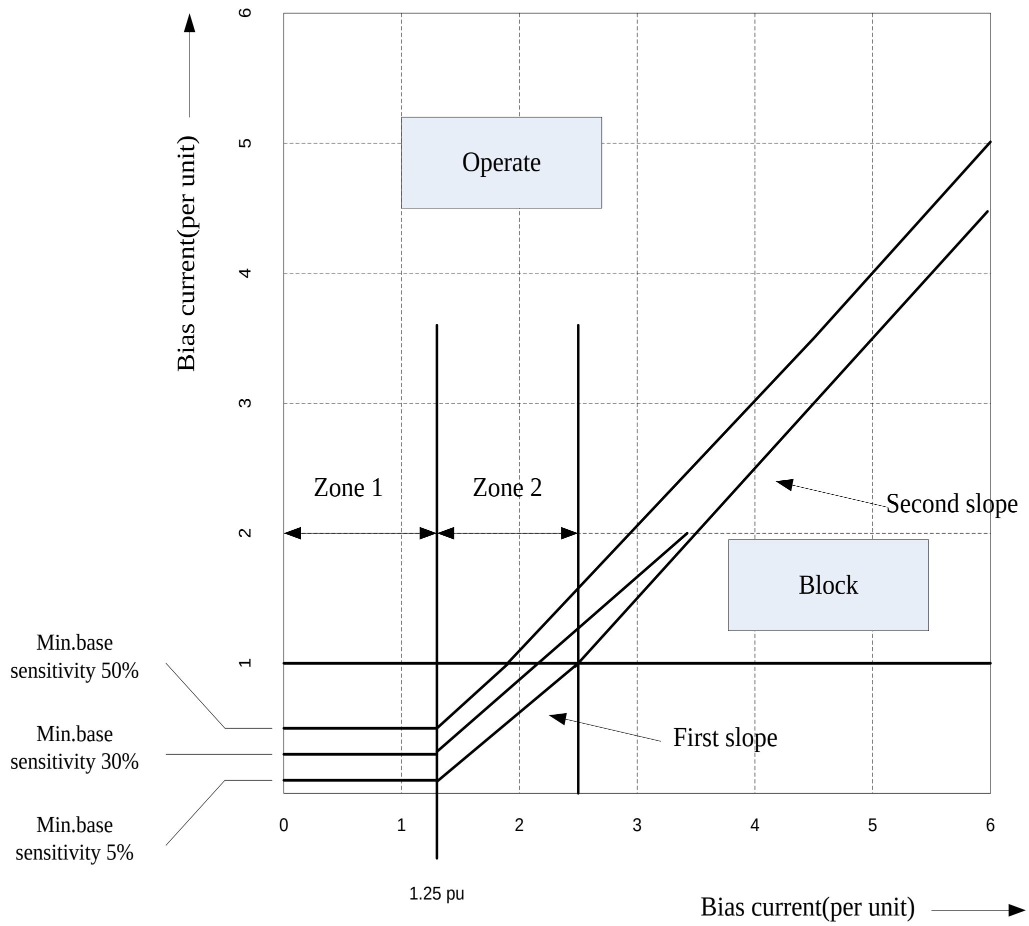


Figure 3.35: Relay characteristic curve (ABB).

This relay has a method to distinguish between internal and external fault. It is called directional check. Directional check is based on RCA which is Relay Characteristic Angle equals to zero. ROA stands for Relay Operating Angle which is between 60 and 90 degree (ABB).

This relay has filters to filter all harmonic components and only fundamental frequency component for mathematical equation that mentioned in section 2.6.5.1 is used. The manual of RET 670 (ABB) page 147, the first part of section 4.2.2.2 mentioned that REF is not sensitive to inrush and over excitation currents and it is only sensitive to the CT saturation. According to the calculations part of this chapter, inrush and over excitation are the most important cause of mal-operation of REF relays.

Like Siemens's relay, this relay needs filters and if one of these filters mal operation, thus relay diagram works wrongly. This relay is fast because each separate parts do their works.

The most noticeable part is this relay work on fundamental frequency of zero sequence. If there is a condition of a fake zero sequence like ct saturation on the sever external earth fault, this algorithm will not operate correctly. Also according to the relay operation diagram steps at part 6, this relay at external earth fault is desensitized, thus if sever external earth fault causes internal earth fault in the same condition relay should operate but it does not operate.

## 3.10 New restricted earth fault (AREVA T&D)

Part (II) of (Tan & Wei, 2007), the equation 2.39 for $I_{diff,G}$ is wrong. According to the IEEE standard (IEEE, 2008a), page 12 and 32, in the definition of $I_{diff,G}$ it does not use maximum of three phase for making residual current. This paper uses wrong equation and it approves that the best and new equation is equation that already mentioned in (IEEE, 2008a).

In part (II), this paper mentions that conventional algorithm for restricted earth fault protection is subjected by CT saturation with high dc of external earth fault. But in part (III) section B mentions that this algorithm also needs separated filters. It shows that this algorithm is like Siemens or ABB algorithm.

Furthermore, when one slope is chosen, it means area in duration that differential current is more than pickup current and restraint current is low, is bypassed. It means that this algorithm has security problem. Also from beginning until the end of zone one in relay characteristic curve, the slope is chosen extremely lower than one, it is used for increasing security and sensitivity in the relay for internal fault. On the other hand, in this algorithm this slope has increased more than one (1.05), thus the security and sensitivity severely has been decayed.

## 3.11 Schneider low impedance REF

At the end of (Bertrand, Gotzig, & Vollet, 2001) there are two limitations for the algorithm. First, if there is no earthed neutral point, REF in case of internal earth fault does not operate. The REF theory is just applicable when neutral point is connected to earth. Otherwise without earthed neutral point this protection function is senseless.

Second limitation is, when the neutral point is earthed with neutral coil, the neutral current is lower than the exact values of fault current. But if the neutral CT is chosen correctly, it will be solved.

According to equations 2.50 and 2.49 there are two different restraint currents for internal and external earth fault. Internal and external earth fault should be clarified by restricted earth fault algorithm. This algorithm has two restraint currents, thus the security of this relay is very low. According to the relay characteristic curve, it has fixed slope (1.05) for correct operation under saturated CT, but this fixed slope decreases the relay sensitivity.